NOTES AND CORRESPONDENCE

Sensitivity of Tropical Rainfall to Banda Sea Diffusivity in the Community Climate System Model

MARKUS JOCHUM

National Center for Atmospheric Research, Boulder, Colorado*

JAMES POTEMRA

International Pacific Research Center, University of Hawaii at Manoa, Honolulu, Hawaii

(Manuscript received 11 September 2007, in final form 23 May 2008)

ABSTRACT

Several observational studies suggest that the vertical diffusivity in the Indonesian marginal seas is an order of magnitude larger than in the open ocean and what is used in most ocean general circulation models. The experiments described in this paper show that increasing the background diffusivity in the Banda Sea from the commonly used value of 0.1 $cm^2 s^{-1}$ to the observed value of 1 $cm^2 s^{-1}$ improves the watermass properties there by reproducing the observed thick layer of Banda Sea Water. The resulting reduced sea surface temperatures lead to weaker convection and a redistribution of precipitation, away from the Indonesian seas toward the equatorial Indian and Pacific Oceans. In particular, the boreal summer precipitation maximum of the Indonesian seas shifts northward from the Banda Sea toward Borneo, which reduces a longstanding bias in the simulation of the Austral–Asian Monsoon in the Community Climate System Model. Because of the positive feedback mechanisms inherent in tropical atmosphere dynamics, a reduction in Banda Sea heat loss of only 5% leads locally to a reduction in convection of 20%.

1. Introduction

The Maritime Continent at the western edge of the Pacific Ocean represents a key region for the Walker circulation, and the overlying atmosphere is characterized by strong precipitation, convection, and low-level wind convergence. This can be attributed to the high sea surface temperatures (SSTs) in the Indonesian seas, which provide a significant source of energy to the atmosphere (e.g., Palmer and Mansfield 1984; Barsugli and Sardeshmukh 2002). Thus, the SST in this region exerts a strong influence on the Walker cell and the Austral–Asian monsoon.

* The National Center for Atmospheric Research is sponsored by the National Science Foundation.

Corresponding author address: Markus Jochum, National Center for Atmospheric Research, 1850 Table Mesa Dr., Boulder, CO 80305.
E-mail: markus@ucar.edu

DOI: 10.1175/2008JCLI2230.1

For the present study, the Java, Flores, and Banda Seas (from here on the sum of all three will simply be referred to as Banda Sea; see Fig. 1) are of particular interest, because several observations suggest strong vertical mixing there with potentially large impact on SST and atmospheric convection (Ffield and Gordon 1992, 1996; Hautala et al. 1996). This increased mixing is typically accounted for by the breaking of internal tides and strongly sheared flow over sills. Atmosphere data provide strong evidence for the connection between Banda Sea SST and tropical precipitation (Fig. 1): With SST anomalies leading precipitation anomalies by 4 months, the regions of high correlation are in the Maritime Continent region (positive correlation), the central equatorial Pacific, and East Africa (negative correlation). Therefore, warmer-than-normal SST in the Banda Sea is followed by increases in rainfall in the Java Sea and eastern Indian Ocean and a decrease in rainfall in the central Pacific and East Africa. This is consistent with Banda Sea SSTs contributing to the Walker cell; increases in SST correlate with local in-

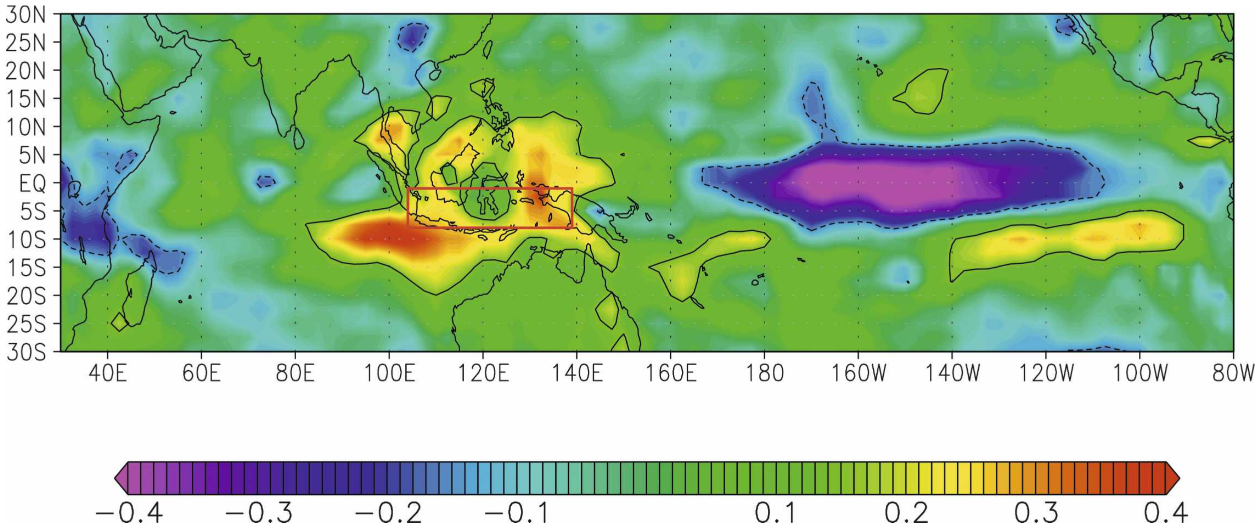

FIG. 1. Correlation of SST anomalies (relative to the climatology of the seasonal cycle) in the Java, Flores, and Banda Seas (region outlined with box) to precipitation anomalies 4 months later (based on NCEP; Kalnay et al. 1996). The correlation for the 95% confidence interval (=0.15) is marked with a black contour line.

creases in convection and increasing subsidence in the remote central Pacific.

It has been shown in an ocean general circulation model (OGCM) that tidal mixing can directly affect SST in the Banda Sea (by approximately 0.3°C; Schiller 2004), and it has been shown in observations that there is SST and atmospheric variability on tidal frequencies (Loder and Garrett 1978; Balling and Cerveny 1995; Ray 2007). What has been lacking so far is the demonstration that in a coupled general circulation model (GCM) the atmospheric general circulation model is sensitive to the small SST changes caused by tidal mixing. The present study not only demonstrates this sensitivity, but it also shows that realistic Banda Sea diffusivity in a GCM leads to improved precipitation and watermass properties. The next section describes the experiments in detail, and section 3 describes the results, which are then discussed in section 4.

2. Model description and experimental setup

The GCM is the latest version of the Community Climate System Model (CCSM3), in its T42x1 configuration. The spectral truncation of the atmosphere yields a 2.8° horizontal resolution, and in the ocean the horizontal resolution is nominally 1° with an equatorial meridional refinement to 1/4°. The vertical resolutions for atmosphere and ocean are 26 and 40 layers, respectively. Resolution and parameterizations are within the normal range of current climate models (for details, see Collins et al. 2006).

Within this global system, modeling the climate over the Indonesian seas is arguably one of the biggest challenges, because it requires a realistic representation of land, ocean, and atmospheric processes. Thus, most climate models have significant shortcomings in their simulation of mean and monsoon climate (Kang et al. 2002) for the Indonesian seas. In CCSM3, one of the largest biases throughout the year is a warm SST bias over much of the Indian Ocean and the Indonesian seas, which is accompanied by excessive precipitation (Large and Danabasoglu 2006).

The purpose of the present study is to quantify the effect that an increased vertical diffusivity in the Indonesian marginal seas has on the states of ocean and climate. The vertical diffusivity in CCSM3, the present control (CONT), is determined by the *K*-profile parameterization scheme (Large et al. 1994), which has enhanced diffusivity in areas of low Richardson numbers (mostly near the surface) and everywhere else a low background diffusivity. This background diffusivity is horizontally uniform with values of 0.1 $cm^2\ s^{-1}$ in the upper ocean, and it increases to 1 $cm^2\ s^{-1}$ in the abyss to account for increased vertical mixing near bottom topography.

However, observations suggest that the background diffusivity can vary spatially by two orders of magnitude (e.g., Gregg et al. 2003; Hibiya and Nagasawa 2004). In particular, Ffield and Gordon (1992) and Hautala et al. (1996) suggest for the upper Banda Sea a diapycnal diffusivity of 1–2 $cm^2\ s^{-1}$, an order of magnitude larger than what is commonly used in OGCMs. Most recently, the numerical study on tidal flow in the Indonesian seas by Koch-Larrouy et al. (2007) also suggested an average vertical diffusivity of 1.5 $cm^2\ s^{-1}$.

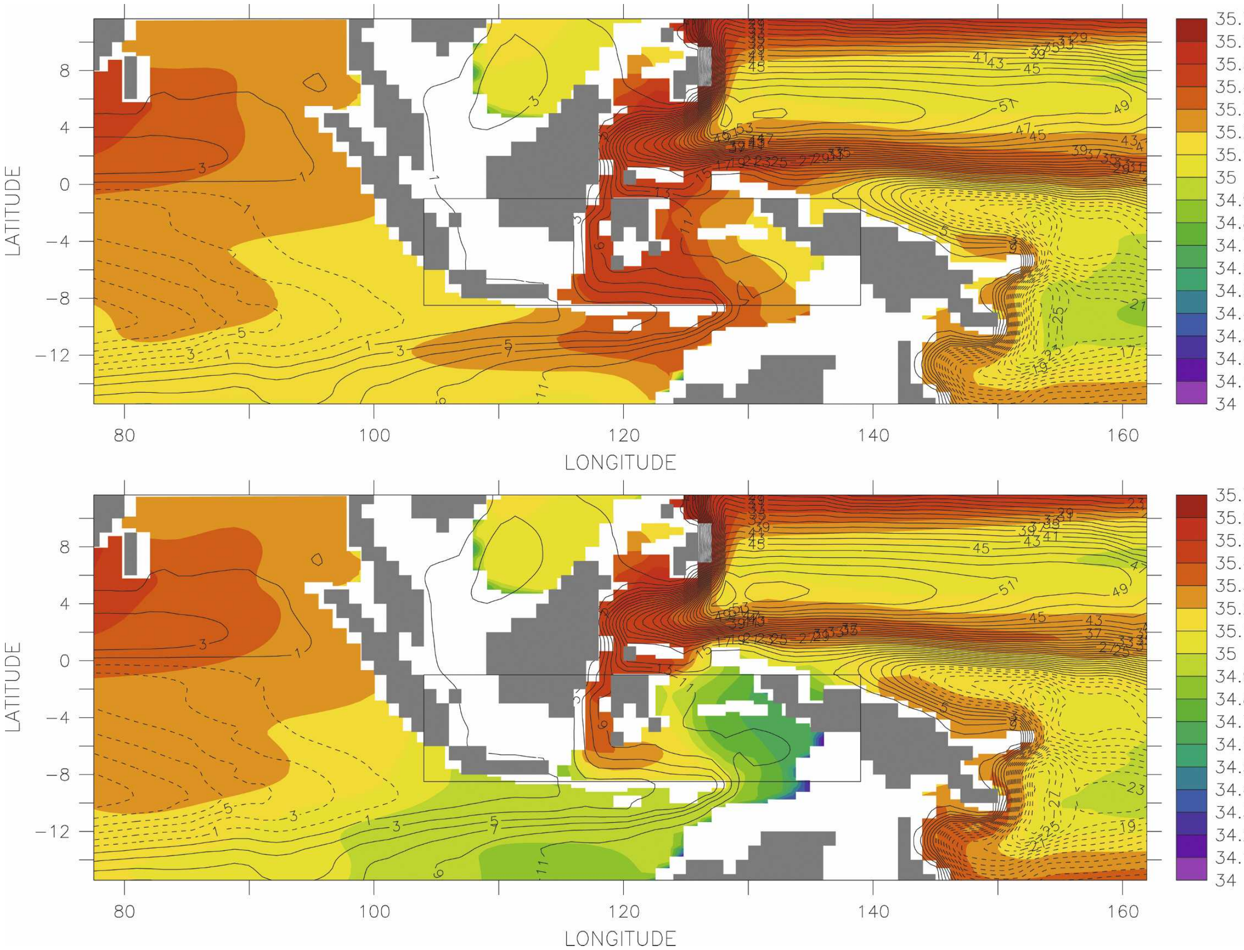

FIG. 2. Maximum salinity between 100- and 500-m depth (color), and mean barotropic streamfunction (contour lines: 2 Sv) for (top) CONT and (bottom) SENS. White indicates water less than 100 m deep; gray indicates land. The region of increased vertical background diffusivity in SENS is outlined with a box in both panels.

The experiment that was performed (SENS) has a setup that is identical to CONT, except that the background diffusivity in the area between 8° and 1°S and 104° and 139°E (mainly Banda, Flores, and Java Seas; Fig. 2) is increased by a factor of 10 to match the observed estimates. CONT and SENS were both integrated for 100 yr, starting from initial conditions based on Levitus et al. (1998). The following results are based on the mean of years 61–100; the significant differences between CONT and SENS are mainly restricted to the seasonal and annual mean fields in the Indo-Pacific domain and are discussed in the next section. Amplitude and spectral characteristics of El Niño are not changed significantly and are therefore not discussed.

3. Results

The Indonesian Throughflow (ITF) is directed from the Pacific Ocean to the Indian Ocean, the dominant route being from the North Pacific via the Mindanao Current through the Makassar Strait (straddling the equator along approximately 119°E; Fig. 2) and Banda Sea into the eastern Indian Ocean (Gordon and Fine 1996). Recent observations suggest an ITF strength of 8.4 ± 3.4 Sv (1 Sv ≡ 10^6 m^3 s^{-1}; Hautala et al. 2001). In both experiments, this pathway is reproduced (Fig. 2), and the ITF transports and their baroclinic structure are almost identical in both, with a transport of 12.4 Sv for CONT and 12.6 Sv for SENS.

Water in the Indonesian seas is sufficiently different from surrounding water to be a unique water mass. Upper-thermocline Pacific Tropical Water (noted by a salinity maximum around 24.5 σ_θ) and lower-thermocline Pacific Intermediate Water (salinity minimum near 26.5 σ_θ) are mixed in the Indonesian seas and become converted into isohaline Banda Sea Water (Wyrtki 1961; Bray et al. 1996; Fieux et al. 1996). North Pacific Intermediate Water (350–1500 m, 4°–10°C) is

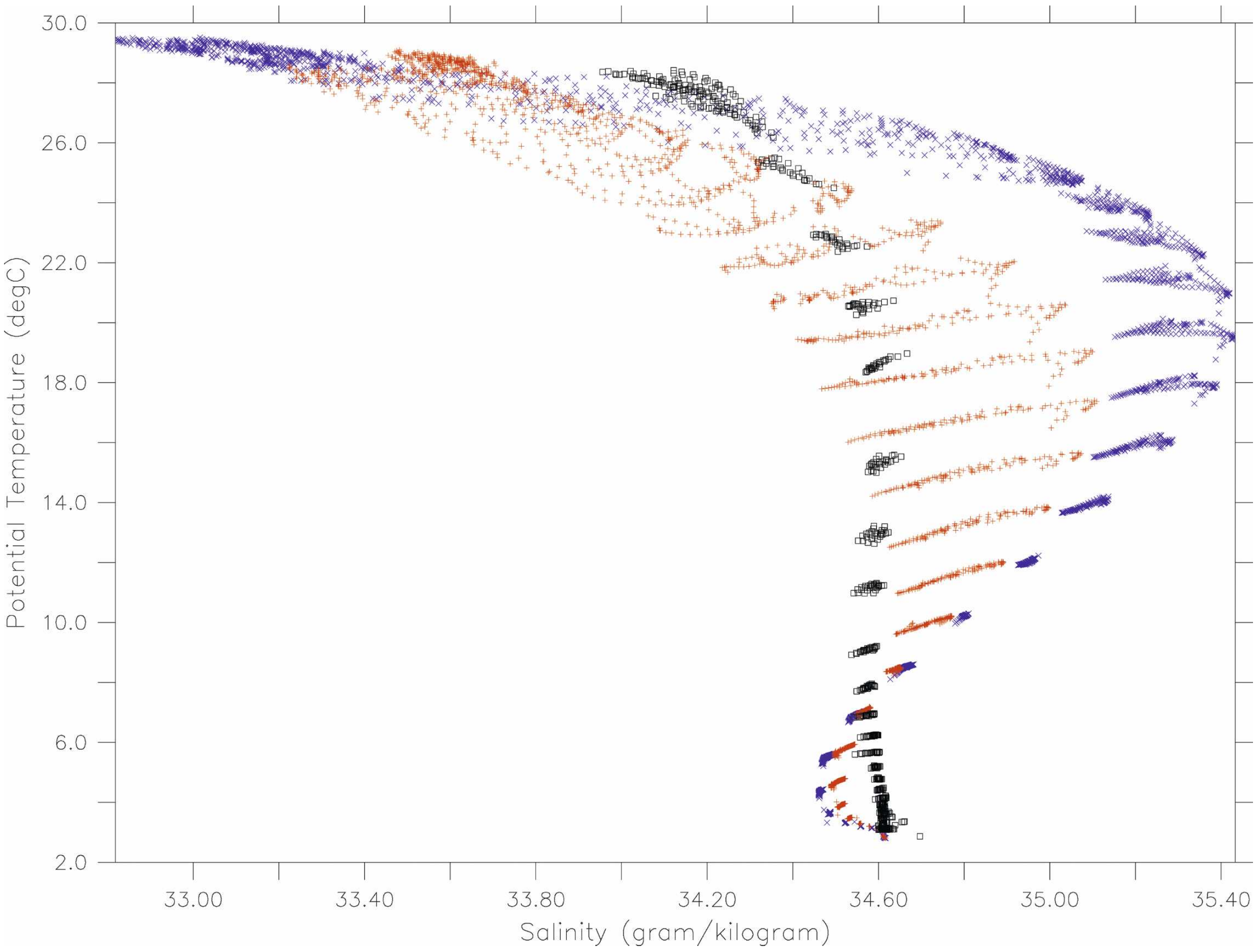

FIG. 3. Temperature–salinity diagram of the Banda Sea based on Levitus et al. (1998) (black squares), CONT (blue crosses), and SENS (red crosses).

characterized by a salinity minimum at 27.4 σ_θ and enters the Banda Sea north of Halmahera, below the isohaline Banda Sea Water (Rochford 1966; van Aken et al. 1988; Coatanoan et al. 1999).

The effects of mixing in SENS are illustrated by following the maximum salinity water of the North Pacific upper thermocline along the streamlines into the Indian Ocean (Fig. 2, bottom): the water keeps its maximum salinity until it enters the Makassar Strait and Banda Sea, where the enhanced diffusivity reduces its salinity. This is in contrast to CONT, where the water maintains its high-salinity signature all the way into the Indian Ocean (Fig. 2, top). This leads to an improved salinity distribution in the central Banda Sea (Fig. 3). The observations show a thick layer of isohaline water from 6° to 22°C, whereas in CONT the high-salinity signature of the North Pacific thermocline water is still maintained. Banda Sea Water in SENS is still not isohaline, but the signatures of the individual water masses are weakened. Most important for local climate, though, is that increasing vertical mixing weakened the strong surface stratification. The surface salinities of less than 33 psu and temperatures of more than 29°C have been improved to resemble more the observations of temperatures of 28°C and salinities of larger than 34 psu. The improved watermass properties in SENS suggest that vertical mixing in the Banda Sea is enhanced indeed, which supports the interpretation of the observations by Ffield and Gordon (1992) and Hautala et al. (1996), and corroborates the OGCM results of Schiller (2004) and Koch-Larrouy et al. (2007).

The temporal and spatial means of the SST in the Banda Sea (hereinafter, the Banda Sea is given by the area of enhanced diffusivity) are reduced from 29.6° to 29.3°C (Fig. 4). The standard deviation for the annual mean in both experiments is 0.13°C. The null hypothesis that the Banda Sea SST in SENS is not colder than in CONT can be rejected at the 0.1% level (based on a two-tailed, two-sample t test with 19 independent samples; Wilks 1995). For comparison, the Reynolds

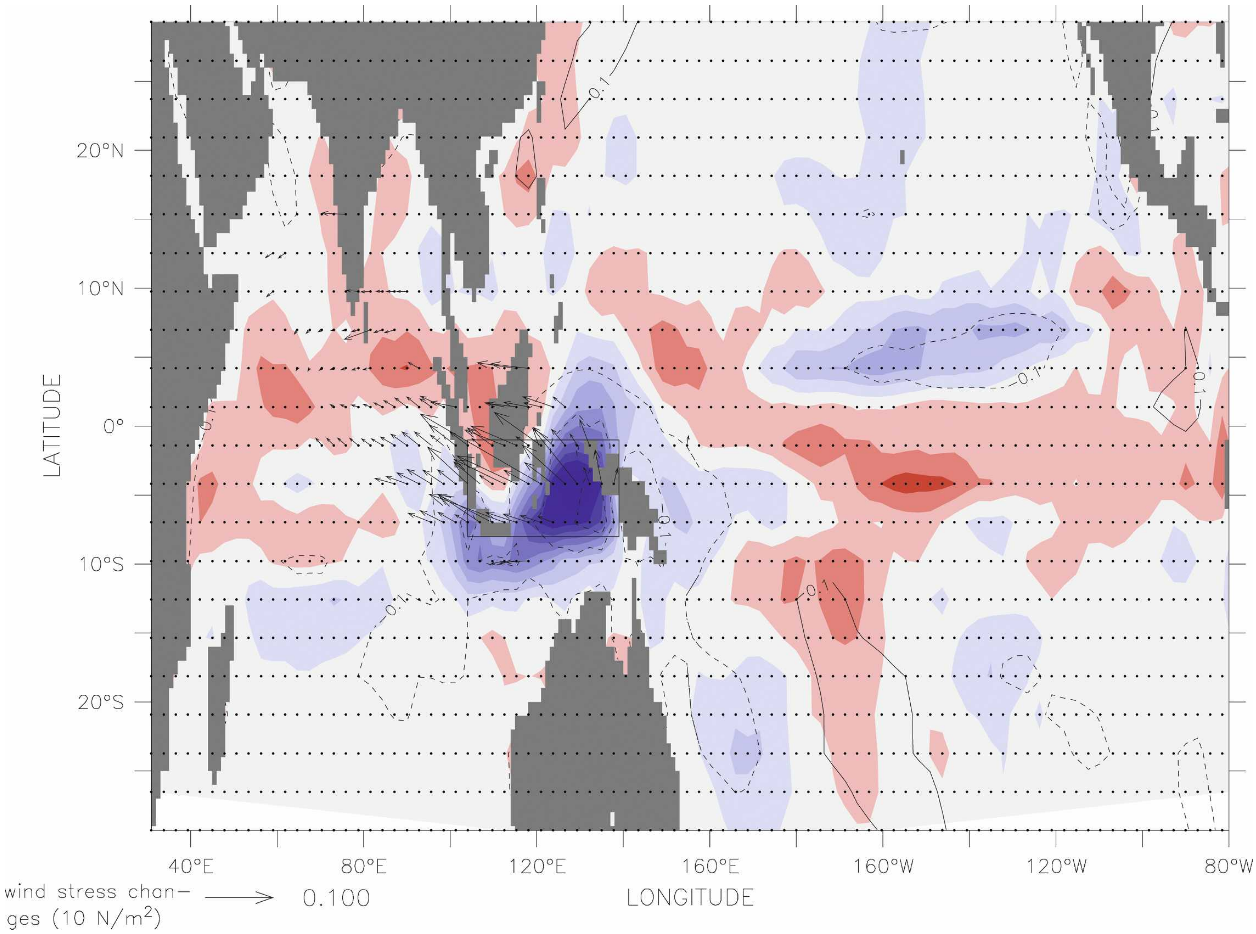

FIG. 4. Differences between SENS and CONT for mean SST (contour lines: 0.2°C), precipitation (color intervals: 0.2 mm day^{-1} beginning at ±0.1 mm day^{-1}), and surface wind stress (for clarity only changes larger than 10% are shown). The dots illustrate the atmospheric resolution and represent a grid point each. The uncertainties for the mean SST are less than 0.1°C and 0.3 mm day^{-1} everywhere in the displayed domain. Thus, all the displayed SST changes present a significant change of the mean, whereas the first level of shading in the precipitation changes (0.1–0.3 mm day^{-1}) is only displayed to highlight the structure of the response. Note, however, that even in the regions that technically do not represent a significant change of the mean precipitation, changes are often collocated with SST changes.

and Smith (1994) data suggest 28.7°C for this area, and data acquired by the Tropical Rainfall Measuring Mission (TRMM) Microwave Imager (Gentemann et al. 2004) suggest 29.3°C. The 0.3°C reduction in SENS is small relative to SST biases of more than 5°C that can be found in coastal upwelling regions or at the boundaries between subpolar and subtropical gyres (Large and Danabasoglu 2006), and is easily within the observational uncertainty (Hurrell and Trenberth 1999). However, because of the nonlinearities governing evaporation and the high SST in the Indonesian seas, the atmospheric response is profound, and the temporal and spatial means of precipation in this area are reduced from 8.7 to 7.6 mm day^{-1} (Fig. 4). The standard deviation for the annual mean in both experiments is 0.4 mm day^{-1}. The null hypothesis that over the Banda Sea it rains not less in SENS than in CONT can be rejected at the 0.1% level (based on a two-tailed, two-sample t test with 19 independent samples; Wilks 1995). Observations (Fig. 1) and theoretical considerations (e.g., Gill 1980) also suggest that reduced SST leads to weaker midtropospheric heating and hence weaker convective activity with potentially global effects. The sensitivity of CCSM3 to these effects is the main result of the present study.

Over the Banda Sea, the midtropospheric convective heating in CONT averages 2.1°C day^{-1} with a maximum of 4.7°C day^{-1} at 500 hPa; the reduced SST in SENS does not change the vertical structure of the heating but reduces its maximum to 4.2°C day^{-1} and its column average to 1.9°C day^{-1} (consistent with the rainfall changes above; Table 1). The reduced atmo-

TABLE 1. Mean Banda Sea values for oceanic and atmospheric variables (see text for details).

Case	CONT	SENS
SST	29.6	29.3
Precipitation (mm day^{-1})	8.7	7.6
Avg tropospheric heat (°C day^{-1})	2.1	1.9
Max tropospheric heat (°C day^{-1})	4.7	4.2
Net shortwave (W m^{-2})	187	193
Net longwave (W m^{-2})	−47	−47
Latent heat (W m^{-2})	−118	−113
Sensible heat (W m^{-2})	−13	−12
Net heat (W m^{-2})	9	21

spheric heating is the result of a changed surface energy budget. The Banda Sea is almost in equilibrium with the overlying atmosphere: in CONT, 187 W m^{-2} incoming shortwave radiation is balanced by 118 W m^{-2} latent heat loss, 47 W m^{-2} longwave radiation, 13 W m^{-2} sensible heat loss, and 9 W m^{-2} ocean heat gain. In SENS, the ocean heat gain increased to 21 W m^{-2}, the additional 12 W m^{-2} coming in equal parts from increased solar radiation and reduced latent and sensible heat loss. Thus, from an oceanic point of view, there is an important atmospheric feedback to increased diffusivity: the reduced SST leads to reduced latent heat loss and therefore reduced cloudiness and increased solar radiation, which in turn is a negative feedback on SST cooling. The reduced SST also leads to a shift in precipitation from the Banda Sea toward the Indian and central Pacific Oceans (Fig. 4). Despite the large local changes in precipitation, the total global precipitation and tropical precipitation are identical in CONT and SENS.

Precipitation is connected to SST through convection, and the center of convection shifts from the northern tip of New Guinea with a maximum annual mean ascent rate ω of 0.11 Pa s^{-1} to Borneo with ω being reduced to 0.9 Pa s^{-1} (both values at 400 hPa). For comparison, the reanalysis products provide maximum values of 0.7 Pa s^{-1} [National Centers for Environmental Prediction (NCEP), just west of Sumatra at 400 hPa] and 0.17 Pa s^{-1} (40-yr European Centre for Medium-Range Weather Forecasts reanalysis, over New Guinea at 500 hPa).

The analysis above suggests that a 5% reduction in oceanic latent heat loss over the Banda Sea leads to a 10% reduction in midtropospheric convective heating, which in turn reduces local convective activity by 20%. The positive feedbacks associated with the latent heat loss can be understood with tropical atmosphere equilibrium dynamics. Convective heating is the equivalent of moisture convergence, and the difference between latent heat loss and convective heating rate has to be due to differences in lateral moisture convergence. Inspection of the model fields show that the change in moisture gradients in this region is negligible (not shown); the wind convergence, however, is reduced indeed (Fig. 4), which is consistent with the linear theory of Gill (1980). One can speculate that the further amplification of the response is tied to a change in stratification: the heating rate is proportional to the product of ascent and stratification ($Q \sim \omega N^2$; Holton 1979). Unfortunately, potential temperature from which to compute the stratification is not saved routinely in CCSM and has to be recomputed from the monthly mean temperature data. Because of the nonlinearities involved, this leads to inaccuracies, and it is not possible here to show that the stratification did indeed increase by 10% as suggested by the amplification between convective heating and convection. However, even the recalculated values show that the annual mean stratification averaged over the Banda Sea is increased in the lower troposphere, albeit only by 3% (not shown).

It is shown here so far that the tropical atmosphere is sensitive to vertical diffusivity in the ocean. The analysis of watermass properties in the Banda Sea strongly suggests that vertical diffusivity should be increased there substantially from the low background values that are currently used in OGCMs. However, based on the change in SST or convective activity alone, it is not clear whether the model climate improved. Evidence for improvement mainly comes from the rainfall changes. For the Banda Sea, the total annual mean rainfall is estimated to be 5.3 [Global Precipitation Climatology Program (GPCP); Xie et al. (2003)], 6.2 (Xie and Arkin 1998), or 6.5 mm day^{-1} (TRMM). Thus, all three observational products suggest that the precipitation in CONT (8.7 mm day^{-1}) is too large and has improved in SENS (7.6 mm day^{-1}). In particular, the June–August (JJA) precipitation over the Banda Sea is much improved (Fig. 5): the CCSM3 biases are largest in the central Pacific (the so-called double ITCZ), the equatorial Atlantic Ocean, and over the southern Indonesian seas. Whereas during JJA the monsoon has a single center over the Bay of Bengal, CCSM3 has a second center over the Indonesian seas, which is removed in SENS. The CCSM3 biases in December–February (DJF) are similar, except for an additional major rainfall bias in the western Indian Ocean (Fig. 6). Over the Indonesian seas the center of the monsoonal rains in CONT is shifted east, which is remedied in SENS. The JJA changes in the Banda Sea are improvements with respect to the three data products analyzed above, whereas the DJF changes are improvements in GPCP and TRMM only.

The differences between the JJA and the DJF re-

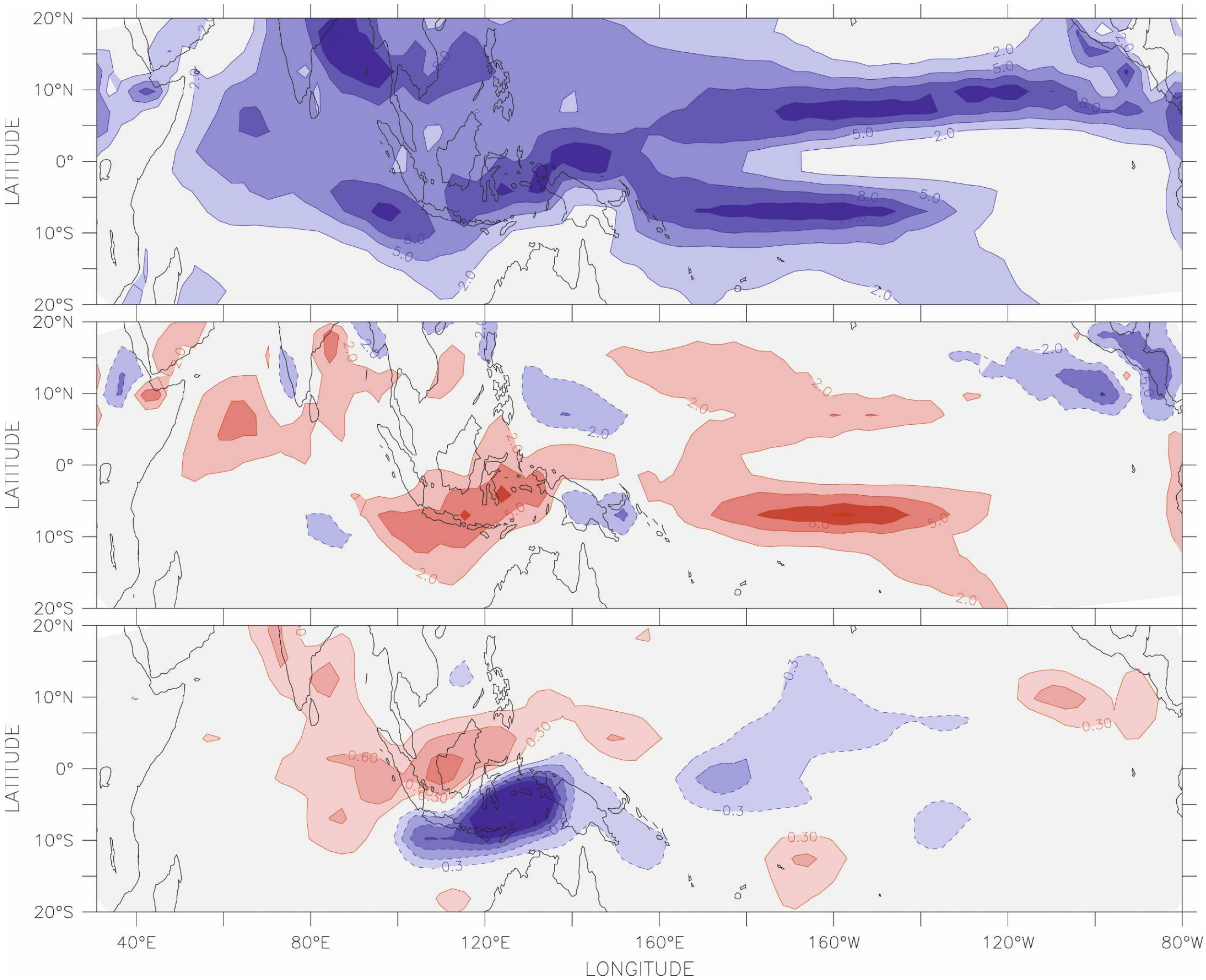

FIG. 5. JJA precipitation rate (mm day^{-1}): (top) CONT (contour intervals: 3 mm day^{-1}, starting at 2 mm day^{-1}), (middle) difference between CONT and observations (GPCP; contour intervals: 3 mm day^{-1}, starting at ±2 mm day^{-1}), and (bottom) difference between SENS and CONT (contour intervals: 0.3 mm day^{-1} between ±1.5 mm day^{-1} and 1 mm day^{-1} beyond that). The largest change is in the Banda Sea with a 3.9 mm day^{-1} reduction.

sponses can be explained by the different background states in these seasons. Banda Sea winds during DJF are weak and southeasterly, whereas during JJA they are stronger and northwesterly (Fig. 7). Thus, in JJA the winds are upwelling favorable in the east Banda Sea, so that the mixed layer shoals and the relatively weak background diffusivity can more easily affect the SST than in DJF with its deeper mixed layer. This results in an SST difference with an average Banda Sea JJA value of 0.39°C and an average DJF value of 0.18°C.

4. Summary and discussion

It has been shown that, in a GCM, tropical precipitation and convection are sensitive to the detailed value of vertical diffusivity in the Banda Sea. Increased diffusivity leads to a cooler SST, reduced latent heat loss, and less diabatic heating and therefore to reduced convection and precipitation. With increased diffusivity, the rainfall in JJA shifts northwestward toward the Bay of Bengal, whereas in DJF it shifts toward the western Pacific warm pool. Because of positive feedback processes in the tropical atmosphere, a 5% drop in latent heat loss over the Banda Sea leads to a 20% reduction of convection.

Because the causal link between diffusivity and convection can be understood with simple equilibrium dynamics, the main contribution of the present study is to demonstrate that at least in one GCM the tropical climate is sensitive to the magnitude of vertical diffusivity. Thus, it is important that the model response can be trusted. Even state-of-the-art GCMs like CCSM3 still

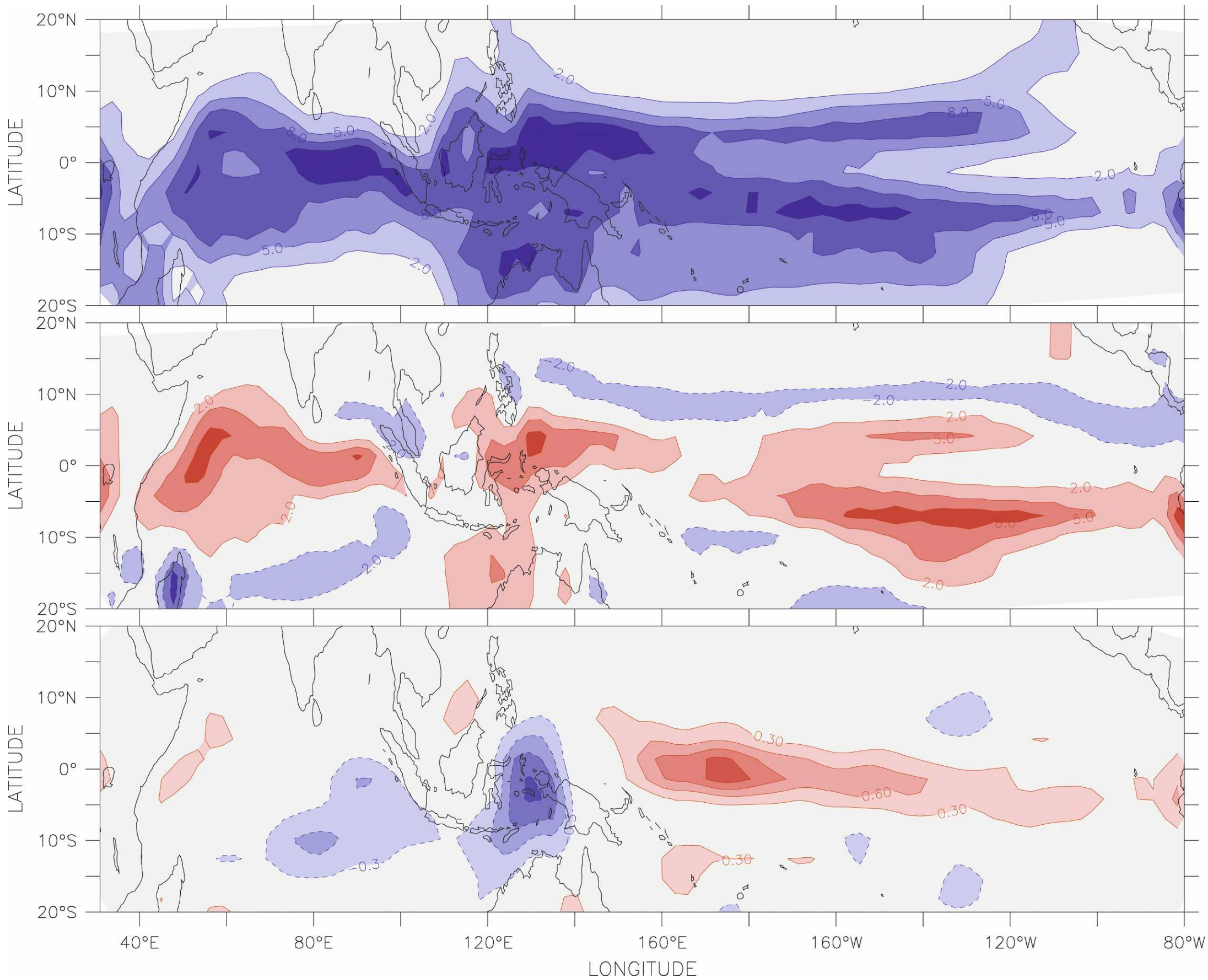

FIG. 6. As in Fig. 5, but for DJF. The largest change is in the Banda Sea with a 1.6 mm day^{-1} reduction.

have biases, the most outstanding of which are probably the precipitation biases in the Indo-Pacific basin (e.g., Large and Danabasoglu 2006): CCSM3 features a spurious double ITCZ in the eastern Pacific with too little precipitation along the equator; it also is too dry over the eastern Indian Ocean and too wet over Indonesia (Figs. 5, 6). However, there are two pieces of evidence to support our interpretation of SENS. First, the pattern of the observed spatial correlation between precipitation and Banda Sea SST anomalies (Fig. 1) matches the pattern of the mean model response (Fig. 4). Second, and more important, increased diffusivity reduces model biases in watermass properties (Fig. 3) as well as in precipitation, which in DJF shifts away from Indonesia toward the central equatorial Pacific (Fig. 6) and in JJA toward the eastern Indian Ocean and Bay of Bengal (Fig. 5). In both seasons, the precipitation shifts toward the warmest SST, which is in the western Pacific warm pool during DJF and in the eastern equatorial Indian Ocean in JJA [in observations (Reynolds and Smith 1994) and in CCSM3]. The precipitation reduction over the Banda Sea during JJA is especially a major improvement in simulating the Austral–Asian monsoon [see Meehl et al. (2006) for a detailed discussion of the monsoon biases in CCSM3].

The sensitivity of tropical precipitation to ocean diffusivity in CCSM3 calls into question the use of horizontally constant diffusivity, which is still used in many OGCMs, and it provides further support to the hypothesis that decadal and shorter-term climate variability could be forced by ocean mixing [see Ray (2007) for a recent discussion]. A long-term goal of GCM development has to be to identify the areas where vertical diffusivity matters and to develop parameterizations for the dominant processes. Although this is mainly theoretical and numerical work, there is clearly the need for

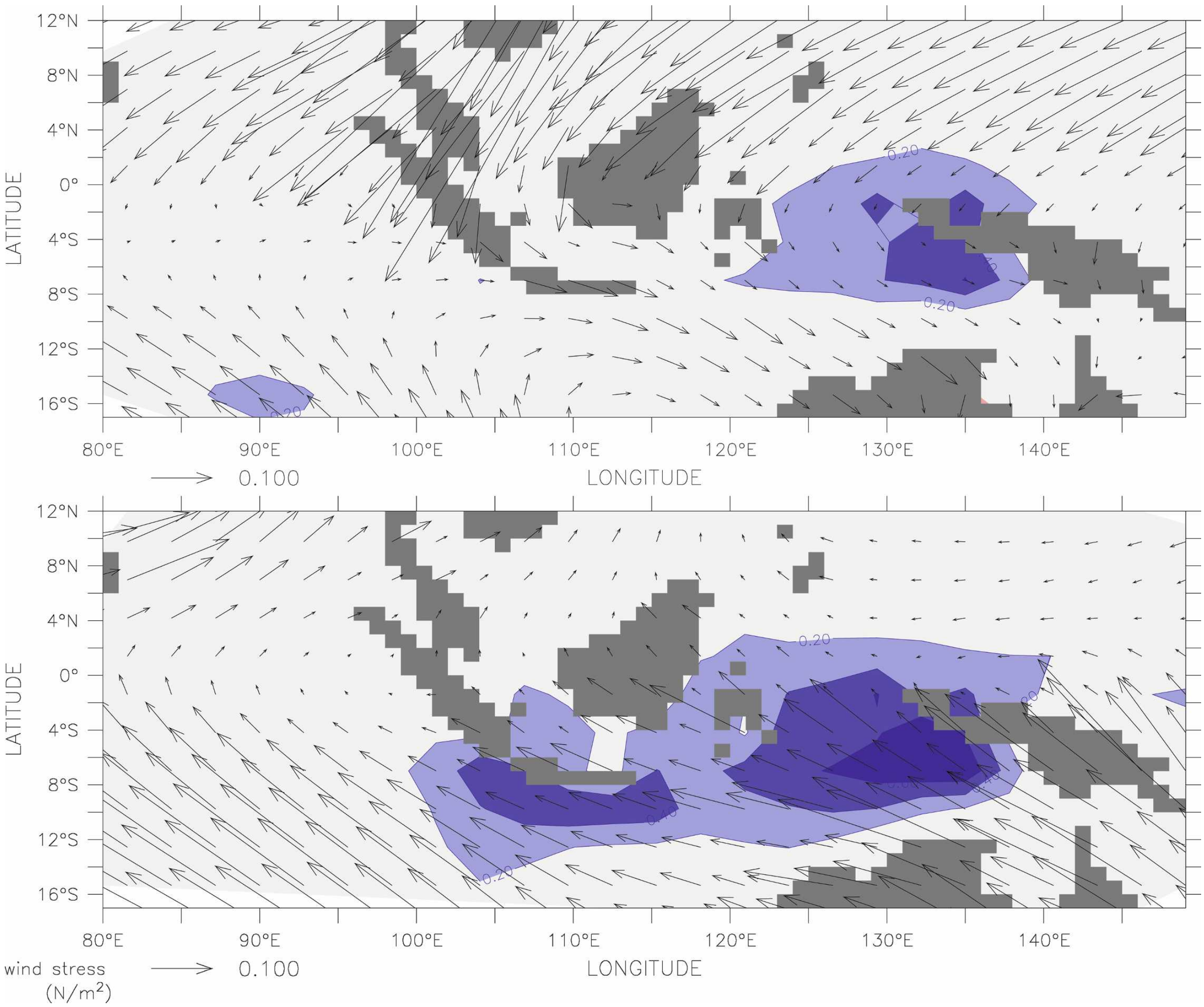

FIG. 7. SST difference between SENS and CONT for (top) DJF and (bottom) JJA, and surface wind stress from SENS for the respective seasons. Contour interval: 0.2°C.

more observational guidance. Inferring vertical mixing from watermass properties is probably only possible in enclosed areas with clearly defined source waters, and the work of Ffield and Gordon (1992) and Hautala et al. (1996) may have been done in one of the few locations where this is possible. Direct microstructure measurements are possible but expensive, and they only provide data at one point over a short period (e.g., Alford et al. 1999). For the tidally induced component of vertical mixing, progress has been made with direct modeling of tides and using observations for validation (Simmons et al. 2004; Koch-Larrouy et al. 2007; Schiller and Fiedler 2007). Modeling the wind-induced part of mixing appears to be more challenging, partly because of the nonlocal structure of the problem and partly because the relevant scales are still being debated (e.g., Nagasawa et al. 2000; Zhai et al. 2007).

Acknowledgments. Author MJ was funded by the National Science Foundation through the National Center of Atmospheric Research (NCAR), and JTP was supported by the Japan Agency for Marine-Earth Science and Technology through its sponsorship of the International Pacific Research Center. This collaboration was made possible through the Faculty Fellowship Program of the Advanced Study Program at NCAR. We are grateful for help and advice from Joe Tribbia, Richard Neale, Grant Branstator, Andrew Gettelman, and Gokhan Danabasoglu. The suggestions of two committed referees improved the manuscript considerably.

REFERENCES

Alford, M. H., M. C. Gregg, and M. Ilyas, 1999: Diapycnal mixing in the Banda Sea: Results of the first microstructure measurements in the Indonesian Throughflow. *Geophys. Res. Lett.,* **26,** 2741–2744.

Balling, R. C., and R. S. Cerveny, 1995: Influence of lunar phase on daily global temperatures. *Science,* **267,** 1481–1483.

Barsugli, J. J., and D. Sardeshmukh, 2002: Global atmosphere sensitivity to tropical SST anomalies throughout the Indo-Pacific basin. *J. Climate,* **15,** 3427–3441.

Bray, N., S. Hautala, J. Chong, and J. Pariwono, 1996: Large-scale sea level, thermocline, and wind variations in the Indonesian throughflow region. *J. Geophys. Res.,* **101,** 12 239–12 254.

Coatanoan, C., N. Metzl, M. Fieux, and B. Coste, 1999: Seasonal water mass distribution in the Indonesian Throughflow entering the Indian Ocean. *J. Geophys. Res.,* **104,** 20 801–20 826.

Collins, W. D., and Coauthors, 2006: The Community Climate System Model: CCSM3. *J. Climate,* **19,** 2122–2143.

Ffield, A., and A. L. Gordon, 1992: Vertical mixing in the Indonesian thermocline. *J. Phys. Oceanogr.,* **22,** 184–195.

——, and ——, 1996: Tidal mixing signatures in the Indonesian seas. *J. Phys. Oceanogr.,* **26,** 1924–1937.

Fieux, M., C. Andrie, E. Charriaud, A. G. Ilahude, N. Metzl, R. Molcard, and J. C. Swallow, 1996: Hydrological and chlorofluoromethane measurements of the Indonesian Throughflow entering the Indian Ocean. *J. Geophys. Res.,* **101,** 12 433–12 454.

Gentemann, C., F. Wentz, C. Mears, and D. Smith, 2004: In situ validation of Tropical Rainfall Measuring Mission microwave sea surface temperatures. *J. Geophys. Res.,* **109,** C04021, doi:10.1029/2003JC002092.

Gill, A., 1980: Some simple solutions for heat-induced tropical circulation. *Quart. J. Roy. Meteor. Soc.,* **106,** 447–462.

Gordon, A., and R. A. Fine, 1996: Pathways of water between the Pacific and Indian Oceans in the Indonesian seas. *Nature,* **379,** 146–149.

Gregg, M. C., T. B. Sanford, and D. P. Winkel, 2003: Reduced mixing from the breaking of internal waves in equatorial waters. *Nature,* **422,** 513–515.

Hautala, S. L., J. L. Reid, and N. Bray, 1996: The distribution and mixing of Pacific water masses in the Indonesian seas. *J. Geophys. Res.,* **101,** 12 375–12 389.

——, J. Sprintall, J. T. Potemra, J. C. Chong, W. Pandoe, N. Bray, and A. G. Ilahude, 2001: Velocity structure and transport of the Indonesian Throughflow in the major straits restricting flow into the Indian Ocean. *J. Geophys. Res.,* **106,** 19 527–19 546.

Hibiya, T., and M. Nagasawa, 2004: Latitudinal dependence of diapycnal diffusivity in the thermocline estimated using a finescale parameterization. *Geophys. Res. Lett.,* **31,** L01301, doi:10.1029/2003GL017998.

Holton, J. R., 1979: *An Introduction to Dynamic Meteorology*. Academic Press, 511 pp.

Hurrell, J. W., and K. E. Trenberth, 1999: Global SST analyses: Multiple problems and their implications for climate analysis. *Bull. Amer. Meteor. Soc.,* **80,** 2661–2678.

Kalnay, E., and Coauthors, 1996: The NCEP/NCAR 40-Year Reanalysis Project. *Bull. Amer. Meteor. Soc.,* **77,** 437–471.

Kang, I., and Coauthors, 2002: Intercomparison of the climatological variations of Asian summer monsoon precipitation simulated by 10 GCMs. *Climate Dyn.,* **19,** 383–395.

Koch-Larrouy, A., and Coauthors, 2007: On the transformation of Pacific Water into Indonesian Throughflow Water by internal tidal mixing. *Geophys. Res. Lett.,* **34,** L04604, doi:10.1029/2006GL028405.

Large, W. G., and G. Danabasoglu, 2006: Attribution and impacts of upper-ocean biases in CCSM3. *J. Climate,* **19,** 2325–2346.

——, J. C. McWilliams, and S. C. Doney, 1994: Oceanic vertical mixing—A review and a model with nonlocal parameterization. *Rev. Geophys.,* **32,** 363–403.

Levitus, S., and Coauthors, 1998: *World Ocean Database 1998*. NOAA Atlas NESDIS 18, 346 pp.

Loder, J. W., and C. Garrett, 1978: The 18.6 year cycle of SST in shallow seas due to variations in tidal mixing. *J. Geophys. Res.,* **83,** 1967–1970.

Meehl, G. A., and Coauthors, 2006: Monsoon regimes in CCSM3. *J. Climate,* **19,** 2482–2495.

Nagasawa, M., Y. Niwa, and T. Hibiya, 2000: Spatial and temporal distribution of the wind-induced internal energy available for deep water mixing in the North Pacific. *J. Geophys. Res.,* **105,** 13 933–13 943.

Palmer, T., and D. A. Mansfield, 1984: Response of two atmospheric general circulation models to SST anomalies in the tropical east and west Pacific. *Nature,* **310,** 483–488.

Ray, R. D., 2007: Decadal variability: Is there a tidal connection? *J. Climate,* **20,** 3542–3560.

Reynolds, R., and T. Smith, 1994: Improved global SST analyses using optimal interpolation. *J. Climate,* **7,** 929–948.

Rochford, D. J., 1966: Distribution of Banda Intermediate Water in the Indian Ocean. *Aust. J. Mar. Freshwater Res.,* **17,** 61–76.

Schiller, A., 2004: Effects of explicit tidal mixing in an OGCM on the water-mass structure and circulation in the Indonesian throughflow region. *Ocean Modell.,* **6,** 31–49.

——, and R. Fiedler, 2007: Explicit tidal forcing in an ocean general circulation model. *Geophys. Res. Lett.,* **34,** L03611, doi:10.1029/2006GL028363.

Simmons, H. L., S. R. Jayne, L. C. S. Laurent, and A. J. Weaver, 2004: Tidally driven mixing in a numerical model of the ocean general circulation. *Ocean Modell.,* **6,** 245–263.

van Aken, H. M., J. Punjanan, and S. Saimima, 1988: Physical flushing of the east Indonesian basins. *Netherlands J. Sea Res.,* **22,** 315–339.

Wilks, D. S., 1995: *Statistical Methods in the Atmospheric Sciences*. Academic Press, 467 pp.

Wyrtki, K., 1961: Physical oceanography of the Southeast Asian waters. NAGA Rep. 2, Scripps Institute of Oceanography, 195 pp.

Xie, P. P., and P. A. Arkin, 1998: Global monthly precipitation estimates from satellite observed outgoing longwave radiation. *J. Climate,* **11,** 137–164.

——, and Coauthors, 2003: GPCP Pentad precipitation analyses: An experimental dataset based on gauge observations and satellite estimates. *J. Climate,* **16,** 2197–2214.

Zhai, X., R. J. Greatbatch, and C. Eden, 2007: Spreading of near-inertial energy in a 1/12° model of the North Atlantic Ocean. *Geophys. Res. Lett.,* **34,** L10609, doi:10.1029/2007GL029895.